DESIGN AND EXPERIMENTAL EVALUATION OF A POSITIONING–CLAMPING POTATO SEED TUBER CUTTING DEVICE
/
定位夹切式马铃薯种薯切块装置设计与试验

Jihao LI [1], Xiangyou WANG*[1], Ranhui ZHU[1]
[1] School of Agricultural Engineering and Food Science, Shandong University of Technology, Zibo 255000,China.
Tel: +86.13806481993; E-mail: wxy@sdut.edu.cn
DOI: https://doi.org/10.35633/inmateh-77-106

Keywords: *potato, potato seed-piece cutting, cutting-and-sectioning device, clamping and flipping, parameter optimization*

ABSTRACT
To address the increasing demand for potato seed-piece cutting and the persistently low level of mechanization dominated by manual operations, an automatic cutting device was designed and developed based on the physical characteristics and agronomic requirements of seed potatoes. Guided by a design strategy that integrates positional clamping with segmented cutting, the system consists of a clamping–feeding module, a flipping unit, and a PLC-based control system. The clamping mechanism secures the positioned tuber, the flipping unit rotates it by 90°, and the PLC coordinates the sequential operations to achieve precise gripping, orientation adjustment, and quartering. Furthermore, the cutting process was analyzed to identify the key factors affecting the quality and uniformity of seed-piece cutting. The qualified cutting rate and blind-eye rate were selected as evaluation indicators, and a three-factor, three-level response surface experiment was conducted using cutter inclination angle, cutting speed, and clamp width as experimental factors. The results indicated that the optimal parameter combination consisted of a cutter inclination angle of 20.7°, a cutting speed of 0.42 m/s, and a clamp width of 15.5 mm, resulting in a qualified cutting rate of 96.66% and a blind-eye rate of 1.85%. All performance indicators met the operational requirements for potato seed-piece cutting.

摘要
对当前马铃薯种薯切块需求大以及以人工切种为主，马铃薯种薯切块机械化程度低等问题，结合种薯的物理特性和农艺要求，基于定位夹取与分段切割的设计思路，研究设计了一种马铃薯种薯自动切块夹取切分装置，通过夹持取料装置完成对定位种薯的夹持，夹持翻转单元实现种薯翻转，PLC 控制各机构动作工序，实现种薯精准夹持、90°翻转及四等分切块的整个切种过程。对马铃薯种薯切块作业过程进行分析，明确该工艺影响种薯切块效果的主要因素。以切种合格率和切种盲眼率为评价指标，以切刀倾斜角、切割速度、夹片宽度为试验因素，进行三因素三水平响应面试验，确定试验最优参数组合。试验结果表明，当切刀倾斜角为 20.7°、切割速度为 0.42m/s、夹片宽度为 15.5mm 时，切种合格率为 96.66%，切种盲眼率为 1.85%，各项性能指标满足马铃薯切种要求。

INTRODUCTION
Seed-piece cutting has become a critical step influencing potato production *(Sasireka et al., 2024; Hang et al., 2025)*. However, manual cutting is characterized by substantial seed-tuber losses, low utilization efficiency, high labor intensity, and elevated production costs, all of which have significantly hindered the advancement of potato mechanization *(Johnson et al., 2023; Wu et al., 2025; Xu et al., 2025)*. Consequently, the development of a highly automated device capable of producing uniform seed pieces has become an essential requirement for achieving fully mechanized potato production.

Most potato seed-cutting machines developed abroad are large-scale integrated systems. The 84-D seed potato cutter developed by Milestone (USA) incorporates a screening mechanism that enables tubers of different sizes to be divided into pieces, but it still produces seed pieces with uneven size. The PGS seed potato cutter produced by Dewulf (Belgium) features a conveying system capable of adjusting tuber orientation during transport and allows continuous disinfection of the cutting blades during operation to ensure seed-piece quality. The Eskel-series potato seed cutters developed by ALL Star Manufacturing & Design LLC in the United States (2019) integrate conveying, grading, cutting, and disinfection into a single system; however, their high cost and inconvenient maintenance limit their applicability.

In China, research and application are still primarily focused on small-scale potato production. *Zhou Shulin (2015)* designed a ladle-type potato seed cutter, but it cannot ensure cutting accuracy and the tubers remain unstable during cutting, resulting in seed pieces with poorly controlled bud-eye distribution. *Zhu Shan et al. (2020)* developed a coordinated longitudinal–transverse blade potato seed cutter; however, the overall cutting quality cannot be reliably ensured. *Feng Wei et al. (2022)* proposed a multifunctional intelligent seed-cutting machine based on potato grading, which combines the cutting mechanism of a ladle-type fixed-blade cutter and uses machine vision to remove seed pieces without bud eyes, thereby improving cutting quality and operational efficiency.

To address these challenges, this study developed a positional clamping–cutting automatic machine for potato seed-piece preparation. Following an analysis of the overall structure and operating principle, the key components of the cutting unit were designed and their structural parameters specified. A mechanical analysis of the entire cutting process was conducted to identify the dominant factors influencing seed-piece cutting performance. In addition, a dedicated test bench was constructed for experimental evaluation. The findings are intended to provide a technical reference for advancing automated potato seed-piece cutting.

MATERIALS AND METHODS

Overall Structure and Operating Principle of the Machine

The automatic seed-cutting system for potato tubers integrates positioning and conveying, clamping and sectional cutting, and disinfection into a single coordinated process. The system comprises a positioning–conveying module, a clamping and feeding mechanism, a cutting assembly, a tuber-piece conveying mechanism, and a centralized control system. The overall system architecture is presented in Fig.1.

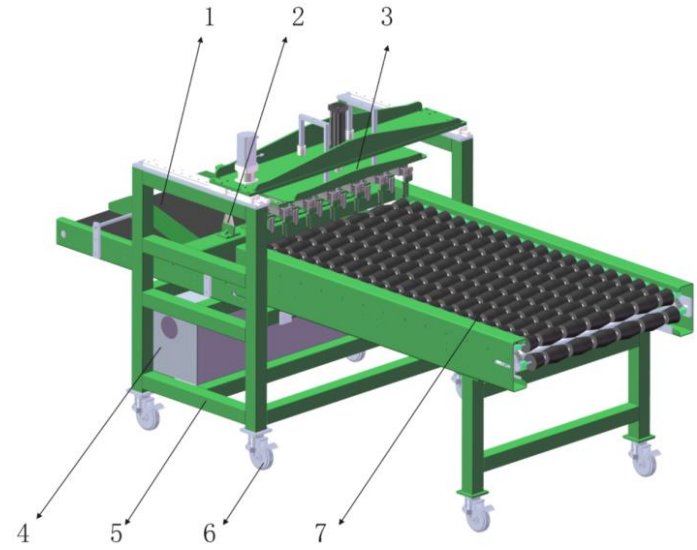

Fig. 1 - Structural schematic of the automatic potato seed-cutting device

1. Potato block conveying unit; 2. Cutting unit; 3. Clamping and feeding device; 4. Electrical cabinet; 5. Frame; 6. Positioning casters; 7. Positioning-conveying unit

First, the positioning-conveying unit transports the seed potatoes and adjusts their orientation through friction generated by a set of frustum-shaped rollers, forming an evenly spaced longitudinal arrangement. A photoelectric sensor located beneath the final roller group detects the arrival of a tuber and transmits a signal to the PLC, which then commands the gripping-feeding mechanism to move forward. The feeding cylinder descends synchronously, and the thin-type gripper cylinder clamps both sides of the short axis of the first-row tubers. Integrated flexible pads enable self-adaptive adjustment of the gripping force, ensuring stable, damage-free holding. Once the magnetic switch of the gripper cylinder confirms a gripping state, the feeding cylinder retracts, and the servo motor receives an acceleration signal from the PLC to drive the tuber towards the double-edged cutter, thereby completing the first cut along the central line of the short axis. When the linear guide slider reaches its terminal position, the PLC receives a signal from the travel-end sensor located at the center of the spring damper and commands the rotary cylinder to perform a 90° flipping motion. The PLC then energizes the solenoid valve to achieve directional switching, after which the servo motor again receives an acceleration signal and drives the gripper at the same speed to carry out the second cut along the central line of the longitudinal axis.

Throughout the entire process, the gripper remains clamped, ensuring that the tuber remains stable without slipping or vibration during cutting. Once the seed potato has been cut, the gripper releases the pieces, which fall through the discharge channel into the collecting unit. The rotary cylinder then resets, the pilot solenoid valve is de-energized, and the system awaits the next batch of tubers for continuous operation.

Design and Analysis of a Positioning–Clamping Potato Seed Cutting Device

The clamping–feeding unit is a key component of the seed potato cutting process. It mainly comprises a rail–slider mechanism, a lifting mechanism, a clamping–rotating mechanism, a cylinder-guided damping mechanism, and a transmission mechanism, as illustrated in Fig. 2(a).

The gripping–flipping unit, serving as the core component of the clamping and flipping mechanism, consists of a thin-type gripper cylinder, a rotary cylinder, grippers, and the connecting flange between cylinders, as shown in Fig. 2(b). The thin-type gripper cylinder actuates the grippers to clamp the geometric center region of the seed potato. Each gripper is composed of two individual clamping plates. To facilitate the first cutting operation when the seed potato passes through the cutter, the clamping plates are made of Q235-A steel with a thickness of 4 mm, and the spacing between adjacent plates in the same direction is set to 6 mm.

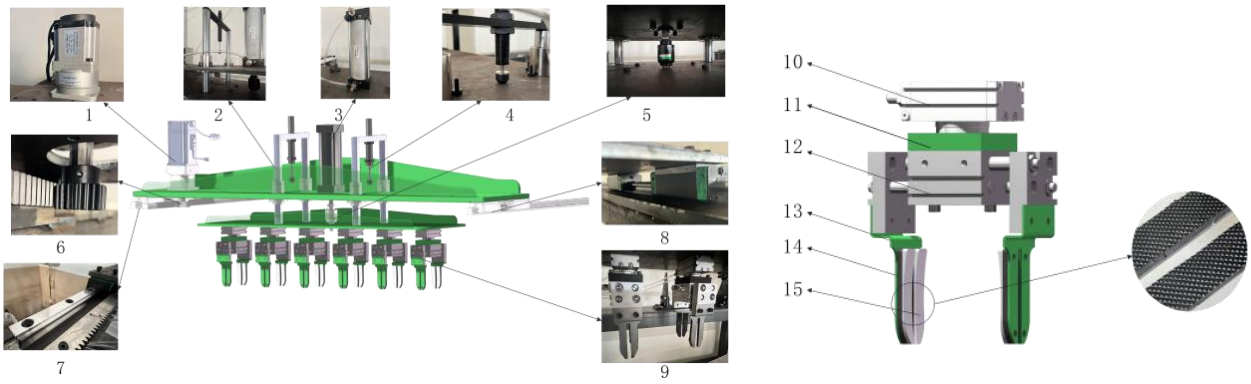

(a) (b)

Fig. 2 - Structural schematic of the clamping and feeding mechanism

1. Servo motor; 2. Moving guide shaft; 3. Feeding cylinder; 4. Hydraulic damper; 5. Universal floating joint; 6. Gear–rack mechanism; 7. Linear guide rail; 8. Guide slider; 9. Clamping-feeding unit;10. Rotary cylinder; 11. Connecting flange; 12. Thin-type gripper cylinder; 13. Gripper plate; 14. Sponge pad; 15. Rubber anti-slip layer. (a). Schematic diagram of the clamping and feeding mechanism;(b). Schematic diagram of the clamping–feeding unit

To ensure that the seed potato does not slip or fall during the entire handling process, a force analysis of the clamping–feeding unit holding the seed potato was conducted, as illustrated in Fig.3.

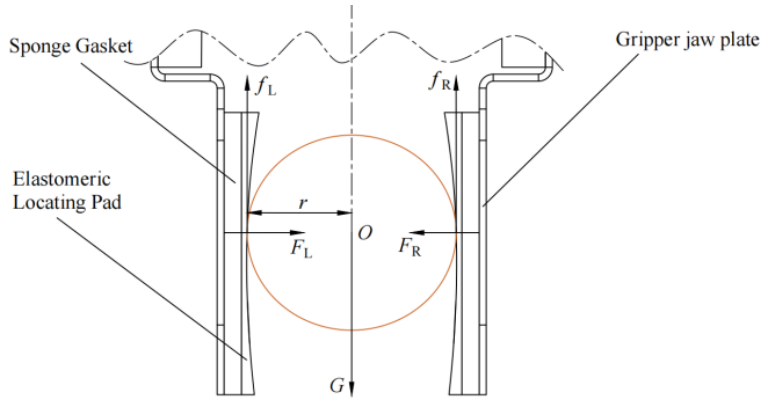

Fig. 3 - Force analysis of the clamping unit during seed potato gripping

For the seed potato to remain stable and prevent slippage during this process, the following condition must be satisfied:

$$\begin{cases} n(f_L + f_R) - G \geq 0 \\ f_L = \mu F_L \\ f_R = \mu F_R \\ rf_L - rf_R = 0 \end{cases} \quad (1)$$

where:

n is the number of clamping fingers; μ is the friction coefficient between the seed potato and the rubber surface of the clamping fingers, 0.4; r is the radius of the potato cross-section, mm; f_L is the friction force acting on the left side of the seed potato, N; f_R is the friction force acting on the right side of the seed potato, N; F_L is the clamping force applied by the cylinder on the left side, N; F_R is the clamping force applied by the cylinder on the right side, N; G is the gravitational force of the seed potato, N.

According to Eq. (1), the seed potato will not slip as long as the total frictional force acting on it is not less than its own weight. To prevent slippage during clamping, conveying, and the moment when the seed potato passes through the cutting blade, a larger safety factor is required. Therefore, a 6-mm-thick layer of high-density sponge was added to the inner surfaces of the grippers to distribute the clamping pressure through elastic deformation and to reduce potential damage to the seed potatoes during operation. In addition, the contact surfaces of the gripper plates were covered with natural rubber, and the rubber surface was designed with corrugated or dotted textures to increase the friction coefficient and prevent slippage. The contact surface was further shaped to conform to the external contour of the seed potato, ensuring better surface conformity during gripping and improving conveying stability.

According to the material characteristics of seed potatoes, a double-edged trapezoidal fixed cutter was designed to facilitate the two-stage cutting process. The cutting assembly consists primarily of the cutter blade, cutter holder, and the mounting plate of the segmentation mechanism. In reference to GB/T 1209.1–2009 Agricultural Machinery—Cutting Components (*China Machinery Industry Federation, 2010*), the cutter was designed with a blade length L_1=90 mm, a blade thickness L_2=1.5 mm, and a blade angle θ=16°. The blade material selected was 9Cr13 stainless steel. Based on agronomic requirements for seed potato segmentation, the cutter is designed to divide each potato into four pieces while preserving the bud eyes.

The seed potato is cut using a sliding-cutting strategy, which effectively reduces the specific cutting resistance and improves the qualified cutting rate *(Yu et al., 2025; Wang et al., 2025)*. As shown in Fig. 4, AB represents the cutting edge of the blade, which moves at a velocity v to perform the cutting operation. Considering an arbitrary point M on the blade edge as a mass point, a force analysis of the sliding-cutting process is conducted.

The dynamic equation of point M during the sliding-cutting operation can be expressed as:

$$\begin{cases} \frac{F_N}{cos\tau} = ma_2 \\ F_N tan\tau - T = ma_1 \\ T = F_N tan\varphi \end{cases} \quad (2)$$

where: m is the mass of particle M, kg; φ is the friction angle between the seed potato and the cutting edge ,°; τ is the shear-slip angle, °; a_1 is the acceleration of the particle relative to the cutter, m·s⁻²; a_2 is the cutting acceleration, m·s⁻²; F_N is the normal force exerted during potato cutting, N; T is the friction force acting on the cutting edge, N.

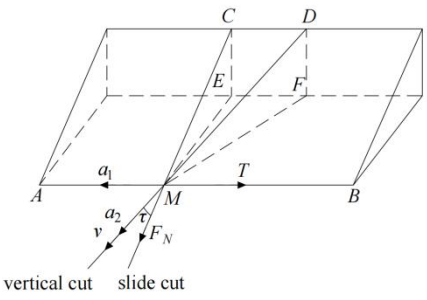

Fig. 4 - Schematic diagram of seed potato shear–slip cutting

For the proposed cutting device, the sliding-cutting angle τ is equal to the blade inclination angle β. According to Eq. (2), a larger β enhances the sliding-cutting effect; however, an excessively large inclination angle also increases the sliding distance and consequently the cutting resistance. Therefore, to ensure both effective cutting performance and acceptable tool life, the blade inclination angle β is constrained within the range of 16° ~24°.

Potatoes exhibit elastoplastic material behavior. When subjected to an impact load, the tuber first undergoes elastic deformation (*Shen et al., 2024*), and once the applied force exceeds its elastic limit, plastic deformation occurs (*Wang et al., 2020*). During this process, local deformation at the contact zone between the seed potato and the blade increases their contact area. A coordinate system is established at the contact point A, where the direction opposite to the linear-guide cutting velocity v is defined as the tangential axis, and its normal direction is defined as the normal axis. The angle α denotes the angle between the impact force F and the cutting velocity v. This angle is identical to the blade inclination angle β, as illustrated in Fig. 5(a).

(a) (b)

Fig. 5 - Schematic diagram for the analysis of the seed potato cutting operation

(a) Force analysis of the seed potato during the first cutting; (b) Force analysis of the tuber block during the second cutting

During the cutting process, the cutting velocity v remains constant, thus:

$$\begin{cases} Ft = mv \\ l = vt \end{cases} \tag{3}$$

where: l is the cutting depth of the blade, mm; F is the impact force exerted by the cutter on the seed potato, N; v is the cutting speed, m/s; β is the blade inclination angle,°; t is the cutting time, s; m is the mass of the seed potato, g.

Assuming that the entire impact load is transmitted to the seed potato during operation, the fracture of the potato under the impact load must satisfy the following dynamic critical condition:

$$F \geq k\sigma_{lim}A \tag{4}$$

where: k is the dynamic correction factor, 1.0; $\sigma_{\lim}$ is the ultimate fracture stress of the potato, Pa; A is the cutting area of the seed potato, mm².

As shown in Fig. 5(b), neglecting the curvature of the contact surfaces between the cutter and the seed potato, the effective contact area produced on the seed potato by the cut is given by *Zhang et al., (2022)*:

$$A = 2lL_2\frac{tan\frac{\theta}{2}}{cos\beta} \tag{5}$$

Based on Eqs. (3)–(5), the critical condition for the fracture of the seed potato can be expressed as:

$$\frac{F}{kA} = \frac{mv^2cos\beta}{2kl^2L_2tan\frac{\theta}{2}} \geq \sigma_{lim} \tag{6}$$

According to Eq. (6), the fracture condition of the seed potato is governed by the cutting velocity v, the blade edge angle θ, and the blade inclination angle β. To ensure effective cutting while minimizing mechanical damage during the process, these parameters must be jointly considered in accordance with the critical fracture condition of the tuber. To satisfy the cutting requirement of seed potatoes, the ultimate stress can be approximated as follows:

$$\sigma_{lim} = \frac{F_{max}}{kA_s} \tag{7}$$

Based on Eqs. (6)–(7), the cutting speed v is required to satisfy:

$$v \geq \sqrt{\frac{2F_{max}l^2L_2tan\frac{\theta}{2}}{kA_smcos\beta}} \tag{8}$$

Potato seed tubers weighing 210–300 g were used in this experiment. The maximum shear force required to completely cut a seed tuber is $F_{\max}$=80 N (*Zhu, 2020*), and full separation occurs at a cutting length of l=80 mm with a cutting cross-sectional area of A_S= 503 mm². According to Eq. (8), the cutting knife can fully cut through the tuber when the cutting velocity satisfies v≥0.387 m·s^{-1}.

As the velocity increases, the cutting force decreases; however, a higher velocity also leads to a stronger impact on the tuber and increases the risk of damage. Based on preliminary tests and the specifications provided in the *Mechanical Design Handbook*, a servo motor integrated with a reduction gearbox was selected, with a rated power of 750 W, a rated speed of 3000 RPM, and a reduction ratio of i=10. Accordingly, the optimal cutting velocity range was determined to be 0.40–0.44 m·s^{-1}.

During the second cutting operation, the gripper is aligned parallel to the cutting knife. The tuber segment is subjected to several forces, including gravity, the clamping force from the gripper, the frictional force between the gripper and the tuber during cutting, and the resistance exerted by the cutting knife. To prevent horizontal slippage caused by the knife–tuber interaction, a force analysis was conducted. An O–XY coordinate system was established with the center of the tuber segment as the origin O, where the X-axis is oriented opposite to the cutting motion and the Y-axis corresponds to the clamping direction of the gripper. The corresponding force analysis diagram is shown in Fig. 5（b）.

The resultant force acting on the tuber segment along the direction of motion is:

$$F_x = f_{L1} + f_{R2} - F_f \tag{9}$$

where: F_f is the friction force between the potato block and the cutter, N.

When the seed tuber is clamped by the biomimetic gripper, local indentation occurs at the contact surface between the gripper and the tuber. The surface rubber anti-slip pad is stretched and deformed, while the sponge layer between the clamping plate and the anti-slip pad is compressed. During the second cutting process, the left and right clamping plates apply equal clamping forces to the tuber. Therefore, the condition for the biomimetic gripper to stably hold the tuber segment during the second cutting operation is:

$$\begin{cases} F_f \le f_{L1} + f_{R2} \\ F_L = A_L(\varepsilon_1 E_1 + \varepsilon_2 E_2) \end{cases} \tag{10}$$

where: A_L is the contact area between the seed potato and a single clamping piece on the left jaw, mm²; ε_1 is the tensile strain of the rubber pad, mm; ε_2 is the compressive strain of the sponge, mm; E_1 is the elastic modulus of the rubber pad, MPa; E_2 is the elastic modulus of the sponge, MPa.

According to Eq. (10), when the moving velocity of the clamping–flipping mechanism is fixed, successful completion of the second cutting operation depends on the contact area between the tuber and the biomimetic gripper. In this experiment, the contact area is mainly determined by the width of a single clamping plate. An excessively large plate width would prevent the gripper from accurately retrieving the tuber from the recess formed by the two truncated-cone rollers, whereas an overly small width would reduce the contact area and increase the likelihood of slippage during cutting. To ensure cutting quality and prevent failures in tuber clamping or slippage during the cutting process, a single-factor experiment was conducted using plate width as the test variable. The results indicated that a plate width of 15 mm provided optimal performance in both clamping stability and cutting quality.

Bench Test

The experiment was conducted in March 2025 at the testing base of Shandong Sidaier Agricultural Equipment Co., Ltd. in Leling, Shandong Province. The potato cultivar Yanshu No.4 was selected as the test material. Seed tubers with an individual mass of 210–300 g were used; they exhibited a quasi-ellipsoidal shape, with measured lengths of 80–100 mm, widths of 65–85 mm, and heights of 60–80 mm. The average moisture content was 74.63%. This cultivar features medium-depth eyes that are relatively uniformly distributed, with a higher density at both ends of the tuber. The cutter inclination angle, cutting speed, and clamping-plate width were selected as the experimental factors. Based on the results of the preliminary single-factor tests, the corresponding ranges were determined as follows: a cutter inclination angle of 16–24°, a cutting speed of 0.40–0.44 m·s^{-1}, and a clamping-plate width of 10–20 mm. This experiment followed the enterprise standard of Shandong Sidaier Agricultural Equipment Co., Ltd., using the cutting qualification rate Y_1 and the blind-eye cutting rate Y_2 as evaluation indices, which were calculated according to Eq. (11).

$$\begin{cases} Y_1 = \dfrac{n_1}{n_0} \times 100\% \\ Y_2 = \dfrac{n_2}{n_0} \times 100\% \end{cases} \tag{11}$$

where:

n_1 is the number of potato blocks with a mass of 40–70 g; n_0 is the total number of potato blocks;

n_2 is the number of potato blocks without any bud eyes.

A three-factor, three-level experiment was designed using the Box–Behnken module in Design-Expert 13. *(Hamid et al., 2024; Dong et.al., 2025)*. The coding of the experimental factors is presented in Table 1.

Table 1

Test factor coding

Code	Cutter inclination angle / °	Cutting speed /m•s^{-1}	Clamp width / mm
-1	16	0.40	10
0	20	0.42	15
1	24	0.44	20

RESULTS

Results and Discussion

The center-point experiment was repeated five times, yielding a total of 17 runs, and the experimental design and results are summarized in Table 2. The data in Table 2 were analyzed using Design-Expert 13 to perform quadratic regression and linear fitting, thereby establishing linear regression models for the cutting qualification rate Y_1 and the blind-eye cutting rate Y_2 as functions of the cutter inclination angle, cutting speed, and clamping-plate width. Significance testing and analysis of variance (ANOVA) were subsequently conducted to identify the key factors influencing cutting performance. The ANOVA results for Y_1 and Y_2 are presented in Table 3.

Table 2

Test protocol and results

Test serial number	X1	X2	X3	Y1 /%	Y2 /%
1	-1	-1	0	90.43	2.74
2	-1	1	0	86.59	3.20
3	0	0	0	97.30	1.69
4	0	0	0	97.41	1.71
5	1	-1	0	88.27	2.56
6	1	0	1	94.63	2.72
7	0	0	0	96.49	1.74
8	0	0	0	96.49	1.65
9	0	-1	1	90.23	2.59
10	1	1	0	91.01	2.35
11	0	1	1	89.18	3.04
12	-1	0	1	93.39	3.05
13	0	-1	-1	89.69	3.13
14	-1	0	-1	90.29	3.28
15	0	1	-1	86.58	2.87
16	1	0	-1	91.62	2.85
17	0	0	0	96.59	1.67

Table 3

Analysis of variance for seed cutting qualification rate and blind eye rate

Indica-tors	Source of variance	Sum of squares	Degree of freedom	Mean square	F	P
Y_1	Model	219.68	9	24.41	54.63	<0.0001***
	X_1	2.92	1	2.92	6.53	0.0378**
	X_2	3.46	1	3.46	7.74	0.0272**
	X_3	10.70	1	10.70	23.94	0.0018***
	X_1X_2	10.82	1	10.82	24.22	0.0017***
	X_1X_3	0.002	1	0.002	0.0045	0.9482
	X_2X_3	1.06	1	1.06	2.37	0.1672
	X_1^2	18.73	1	18.73	41.92	0.0003***
	X_2^2	135.45	1	135.45	303.13	<0.0001***
	X_3^2	21.59	1	21.59	48.31	0.0002***
	Residual	3.13	7	0.4468		
	Lack of Fit	2.29	3	0.7617	3.62	0.1232
	Pure Error	0.84	4	0.2107		
	Cor Total	222.81	16			
Y_2	Model	5.74	9	0.6374	308.69	<0.0001***
	X_1	0.4005	1	0.4005	193.95	<0.0001***

Indica-tors	Source of variance	Sum of squares	Degree of freedom	Mean square	F	P
	X_2	0.0242	1	0.0242	11.72	0.0111**
	X_3	0.0666	1	0.0666	32.26	0.0008***
	X_1X_2	0.1122	1	0.1122	54.35	0.0002***
	X_1X_3	0.0025	1	0.0025	1.21	0.3076
	X_2X_3	0.1260	1	0.1260	61.03	0.0001***
	X_1^2	1.25	1	1.25	603.41	<0.0001***
	X_2^2	0.9560	1	0.9560	462.96	<0.0001***
	X_3^2	2.30	1	2.30	1113.54	<0.0001***
	Residual	0.0145	7	0.0021		
	Lack of Fit	0.0096	3	0.0032	2.62	0.1879
	Pure Error	0.0049	4	0.0012		
	Cor Total	5.75	16			

*Note: *** indicates that the impact is extremely significant (P≤0.01); ** indicates significant impact (0.01<P≤0.05).*

According to Table 3, X_3, X_1X_2, X_1^2, X_2^2, X_3^2 exert extremely significant effects on the cutting qualification rate Y_1, while X_1 and X_2 show significant effects. The remaining factors have no significant influence. The order of influence of the experimental factors on Y_1 is as follows: clamping-plate width, cutting speed, and cutter inclination angle. For the blind-eye cutting rate Y_2, X_1, X_3, X_1X_2, X_2X_3, X_1^2, X_2^2, X_3^2 exhibit extremely significant effects, while X_2 shows a significant effect. The remaining factors are not significant. The order of influence of the experimental factors on Y_2 is as follows: cutter inclination angle, clamping-plate width, and cutting speed. On the premise that the overall models were extremely significant and the lack-of-fit terms were not significant, the nonsignificant terms were removed to refit the models. The resulting multivariate quadratic regression equations for the cutting qualification rate Y_1 and Y_2 the blind-eye cutting rate are as follows:

$$\begin{cases} Y_1 = 96.86 + 0.60X_1 - 0.66X_2 + 1.16X_3 + 1.14X_1X_2 - 0.02X_1X_3 = 0.51X_2X_3 - 2.11X_1^2 - 5.67X_2^2 - 2.26X_3^2 \\ Y_2 = 1.69 - 0.22X_1 + 0.05X_2 - 0.09X_3 - 0.17X_1X_2 + 0.025X_1X_3 + 0.18X_2X_3 + 0.54X_1^2 + 0.48X_2^2 + 0.74X_3^2 \end{cases} \quad (12)$$

As shown in Fig. 6a, Y_1 first increases and then decreases with increasing cutting speed, exhibiting a highly significant effect. Similarly, as illustrated in Fig. 6b, Y_1 also increases initially and then decreases as the cutting speed increases, indicating a highly significant effect. As shown in Fig. 6c, Y_2 decreases first and then increases with the increase in clamping-piece width, showing a highly significant effect. As presented in Fig. 6d, Y_2 also decreases initially and then rises as the clamping-piece width increases, indicating a highly significant effect. The analysis indicates that when the clamping-piece width is excessively large, the seed potato cannot be accurately grasped within the concave pocket of the roller and is more prone to slipping due to dispersed forces, resulting in unstable conveying and cutting performance, which adversely affects both the cutting qualification rate and the blind-eye rate. Conversely, when the clamping-piece width is too small, the insufficient clamping force causes the seed potato to fall off due to inertia during the second cutting operation, thereby reducing the cutting quality. The cutting qualification rate and blind-eye rate are also influenced by the cutting speed. Excessive cutting speed leads to stronger impact forces between the cutter and the seed potato, causing greater mechanical damage and ultimately lowering the cutting qualification rate.

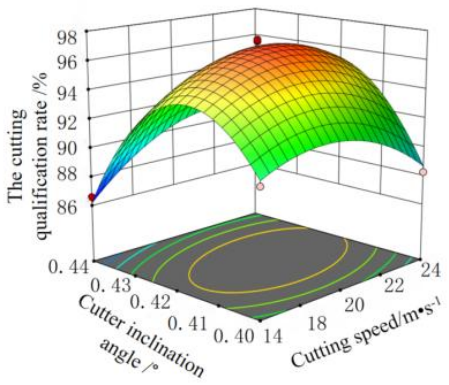

(a). Y_1=(X_1,X_2,15)

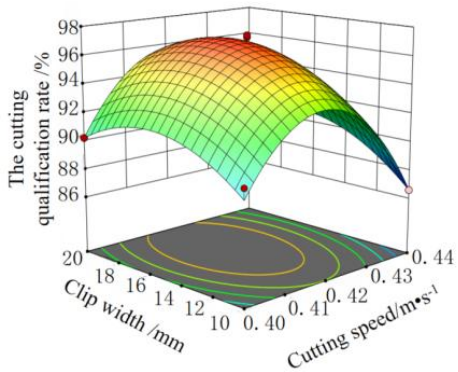

(b). Y_1=(20,X_2,X_3)

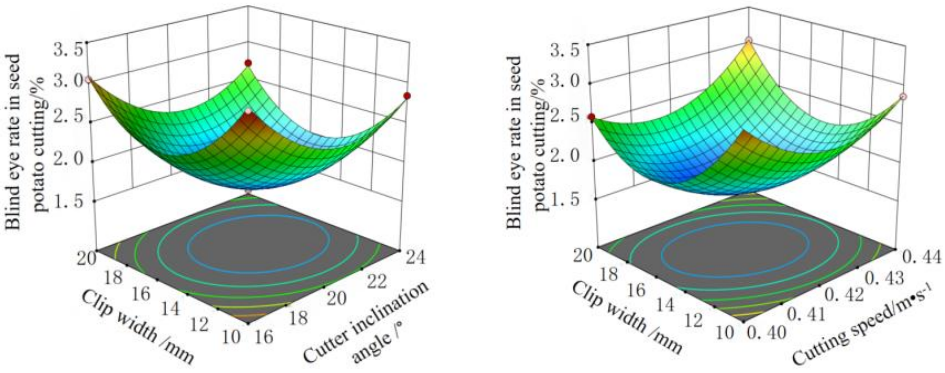

(c). $Y_2=(X_1,0.42,X_3)$ (d). $Y_2=(20,X_2,X_3)$

Fig. 6 - Experimental factor response surface

Using the multi-objective parameter optimization module in Design-Expert 13, the mathematical models were analyzed and solved to obtain several feasible optimal parameter combinations. The optimal combination was determined to be a cutter inclination angle of 20.713°, a cutting speed of 0.419 m/s, and a clamping-plate width of 15.592 mm. Under this parameter setting, the qualified cutting rate of seed potato blocks reached 97.05%, while the blind-eye rate was 1.67%, indicating that the performance fully meets the practical operational requirements.

Experimental Validation

To verify the accuracy of the optimized results and the reliability of the test platform, the parameters obtained from the orthogonal optimization were slightly adjusted. The cutter inclination angle was set to 20.7°, the cutting speed to 0.42 m·s⁻¹, and the clamping-plate width to 15.6 mm. Validation tests were then conducted under this parameter combination, as shown in Fig. 7, with five repeated trials and the average taken. The results showed a cutting qualification rate of 96.66% and a blind-eye cutting rate of 1.85%, corresponding to relative errors of 0.39% and 0.18% from the ideal values, respectively. The experimental results were highly consistent with the predicted values, and both the qualification rate and blind-eye rate met the practical operational requirements. Therefore, this parameter combination can be considered the optimal working condition for potato seed-cutting operations.

(a) (b) (c) (d)

Fig. 7 - Experimental Validation

(a) Potato feeding and clamping; (b) First cutting; (c) Second cutting after flipping; (d) Cutting results

CONCLUSIONS

1) A potato seed-cutting device was developed to achieve fully automated segmentation. In coordination with the alignment and positioning system, the device performs the first cut by clamping and transferring the seed potato to the cutting module. Subsequently, the rotary cylinder drives the gripper cylinder to flip the potato, enabling a second pass through the cutter to complete final segmentation. This sequential clamping–cutting–flipping operation significantly improves seed potato cutting efficiency and substantially reduces manual labor requirements.

2) By constructing a mechanical model of the potato–cutter interaction, the cutting process was analyzed to identify the primary factors influencing cutting quality and their acceptable parameter ranges. The results showed that the factors affecting the qualified cutting rate, in descending order of influence, are clamping-plate width, cutting speed, and cutter inclination angle. In contrast, the dominant factors influencing the blind-eye rate are cutter inclination angle, clamping-plate width, and cutting speed, in that order.

3) Bench tests conducted under the optimal parameter combination demonstrated that when the cutter inclination angle was 20.7°, the cutting speed was 0.42 m/s, and the clamping-plate width was 15.5 mm, the qualified cutting rate reached 96.66%, while the blind-eye rate was only 1.85%. These results confirm that the proposed potato seed-cutting device meets the operational requirements for seed potato segmentation under optimized conditions.

ACKNOWLEDGEMENT

This study was supported by the Major Applied Agricultural Technology Innovation Project of Shandong Province (SD2019NJ010).

REFERENCES

[1] Anno. (2019). *All Star Manufacturing & Design LLC*. http://www.allstarm fgllc.com/2019.

[2] Anno. Milestone. (2019). http://www.milestone-equipment.com/cutters-and- treaters/2019

[3] China Machinery Industry Federation; National Technical Committee for Standardization of Agricultural Machinery. (2010). *Agricultural Machinery—Cutting Devices*. China Standards Press, Beijing/China, GB/T 1209.1–2009, pp. 9–11.

[4] Dewulf. https://www.dewulf.com/

[5] Dong L., Dong X.Y., Wang T., Wang S. (2025). Optimisation of Spraying Parameters for Boom Sprayers. *International Journal of Applied Science*, vol. 8, no. 2, pp.50-58. DOI: https://doi.org/10.30560/ijas.v8n2p50

[6] Feng W., Li P., Zhang X.F., Zhong W.R., Wang P., Cui J.B. (2022). Design and Experiment of Intelligent Cutting Machine for Potato Seed (马铃薯种薯智能切块机设计与试验), *Journal of Agricultural Mechanization Research*, vol.44, no.12, pp.124-129, 134. Beijing/China. DOI: 10.13427/j.cnki.njyi.2022.12.029

[7] Hamid E.A., Amer A.M., Mokbl E.M., Hassan M.A., Amin R.H., Tharwat K.M. (2024). Box-Behnken design (BBD) for optimization and simulation of biolubricant production from biomass using aspen plus with techno-economic analysis. *Scientific reports*, vol.14 pp.1-20. DOI: https://www.nature.com/articles/s41598-024-71266-w

[8] Hang J., Yi F.X., Cui Y.J., Wang X.Y., Jin C.Q., Cheein F.A. (2025). Design and implementation of a seed potato cutting robot using deep learning and delta robotic system with accuracy and speed for automated processing of agricultural products, *Computers and Electronics in Agriculture*, vol.237. DOI: https://doi.org/10.1016/j.compag.2025.110716

[9] Johnson C.M., Cheein F.A. (2023). Machinery for potato harvesting: a state-of-the-art review. *Front Plant Sci,* vol.5 no.14, pp.1-17.DOI: 10.3389/fpls.2023.1156734

[10] Sasireka R., Tenzing D., Himanshu A. (2024). Hydroponics: Exploring innovative sustainable technologies and applications across crop production, with Emphasis on potato mini-tuber cultivation. *Heliyon*, vol.10 no.5: e26823. DOI：10.1016/j.heliyon.2024.e26823

[11] Shen Y., Hu H.B., Xu G.T., Chen Q., Zhou M.G., Zhang C. (2024). Experiment on elastoplastic mechanical properties and damage analysis of potato (马铃薯的弹塑性力学特性试验及其损伤分析), J*ournal of Agricultural Mechanization Research*, vol.46, no.8, pp.174-178,185. Beijing/China. DOI: 10.13427/j.cnki.njyi.2024.08.003

[12] Wang H.Y., Ji Z.L., Zhao X., You Y., Wang D.C., Fang X.L. (2025). Design and Experiment of Forage Harvester Chopper Shape for Bionic Beaver Lower Door Teeth Shape Structure (基于河狸下门齿外形结构的青饲料切碎弯刀设计与试验), *Transactions of the Chinese Society for Agricultural Machinery*, vol.56, no.6, pp.386-396,408. Beijing/China. DOI: 10.6041/j.issn.1000-1298.2025.06.036

[13] Wang L.J., Zhang Z.H., Liu T.H., Wang Y.J., Jia F., Jiang J.X. (2020). Design and experiment of chopping and splitting stalk crushing device for corn harvester header (玉米收获机割台砍劈式茎秆粉碎装置设计与试验), *Transactions of the Chinese Society for Agricultural Machinery,* vol.51, no.7, pp.109-117. Beijing/China. DOI: 10.6041/j.issn.1000-1298.2020.07.013

[14] Wang X.Y., Zhu S., Li X.Q., Li T.X., Wang L.L., Hu Z.X. (2020). Design and Experiment of Directional Arrangement Vertical and Horizontal Cutting of Seed Potato Cutter (定向排列纵横切分马铃薯种薯切块机设计与试验), *Transactions of the Chinese Society for Agricultural Machinery*, vol.51, no.6, pp.334-345. Beijing/China. DOI: 10.6041/j.issn.1000-1298.2020.06.036

[15] Wu Y.S., La X.M., Liu F., Yan J.G. (2025). Design and Performance Testing of Seed Potato Cutting Machine with Posture Adjustment, *MDPI Agriculture,* vol.15 no.7, pp.732-749.DOI: https://doi.org/10.3390/agriculture15070732

[16] Xu R.Z., Chen C., Liu F.Y., Xie S.Y. (2025). Intelligent 3D Potato Cutting Simulation System Based on Multi-View Images and Point Cloud Fusion. *MDPI Agriculture*, vol.15 no.19, pp.2088-2099. DOI: https://doi.org/10.3390/agriculture15192088

[17] Yu S.Y., Hu Z.Q., Yang K., Peng B.L., Zhang Y.H., Yang M.J. (2021). Operation Mechanism Analysis and Parameter Optimization of Garlic Root Floating Cutting Device (大蒜收获机浮动切根装置作业机理分析与参数优化), *Transactions of the Chinese Society for Agricultural Machinery*, vol.52, no.5, pp.111-119. Beijing/China. DOI: 10.6041/j.issn.1000-1298.2021.05.012

[18] Zhang Z.G., Zhao M.Y., Xing Z.Y., Liu X.F. (2022). Design and experiment of dual-action opposing cutting end-effector for safflower harvester (红花采收机双动对切式末端执行器设计与试验), *Transactions of the Chinese Society for Agricultural Machinery,* vol.53, no.12, pp.160-170. Beijing/China. DOI: 10.6041/j.issn.1000-1298.2022.12.015

[19] Zhou S.L., *Coop-type fixed-blade seed potato cutting machine*. Patent. No. 201510180121.3, China.

[20] Zhu S. (2020). *Design and experiment of the seed potato cutting machine*, MSc Thesis, Shandong University of Technology, Zibo/China.